Liu, W. and Chen, Q. 2015. "Optimal air distribution design in enclosed spaces using an adjoint method," *Inverse Problems in Science and Engineering*, 23(5), 760-779.

Optimal air distribution design in enclosed spaces using an adjoint method

Wei Liu[b,a], Qingyan Chen[a,b,]*

[a] School of Mechanical Engineering, Purdue University, West Lafayette, IN 47907, USA;
[b] School of Environmental Science and Engineering, Tianjin University, Tianjin 300072, China

This investigation studied an adjoint method to achieve the optimal design of ventilation in an enclosed environment and validated it with two, two-dimensional cases. A part of the flow field and/or temperature field was defined as the design objective, and the thermo-fluid boundary conditions were determined as the design variables. By using the adjoint method together with a steepest descent method that was implemented in OpenFOAM, this investigation found the optimal air supply parameters. With the determined air supply parameters, this study used CFD to calculate the flow and/or temperature fields, which are in a good agreement with the design objective. However, as the adjoint method could only find the local optima, the calculations with different initial inlet air conditions may lead to multiple optimal solutions. This is common with the gradient-based method.

Keywords: inverse design, optimal control, ventilation, inlet boundary conditions, adjoint methd

1. Introduction

Ventilation is one of the most important factors in maintaining an acceptable indoor environment in enclosed spaces such as buildings and transportation vehicles. Ventilation can control the air temperature, relative humidity, air speed, and chemical species concentrations in the air of enclosed spaces. There are many standards [1] for formulating the requirements of an indoor environment, and ventilation design should be optimized for creating and maintaining an environment to satisfy the requirements.

Traditionally, researchers and engineers have applied a "trial-and-error" process in designing ventilation, which means predicting and evaluating ventilation performance with different design variables to find the scenario that best agrees with the design objective. According to Chen [2], researchers and engineers have typically predicted or evaluated ventilation performance by analytical and empirical models, experimental measurements, and computer simulations. With the development of computer technology, Computational Fluid Dynamics (CFD) simulations have recently been the most popular method of predicting ventilation performance. A CFD simulation can provide field distributions of air velocity, air temperature, species, etc. With a validated turbulence model, a CFD simulation would be more accurate and informative than analytical models, empirical models, multizone models, and zonal models and much faster than experimental measurements. However, because this "trial-and-error" process requires CFD simulations for a large number of scenarios, it would take days or months to obtain an optimal design for a ventilated space. At the same time, a "trial-and-error" process with the other methods may be inaccurate, non-informative, expensive, and/or time-consuming. Most importantly, because of the subtlety and complexity of fluid flow, it is unlikely that repeated trials in an interactive analysis and design procedure would lead to a truly optimal design. By eliminating the notion of this "trial-and-error" process, the optimization approach could achieve this design goal.

The optimization approach has been widely applied in identifying a groundwater pollution source, in a linear optimization method [3], maximum likelihood method [4], and nonlinear

*Corresponding author. Email: yanchen@purdue.edu

optimization method [5]. Generally, there are two main categories of optimization approach: the gradient-based method and the gradient-free method. The gradient-free method such as Genetic Algorithms (GA) [6] uses a population of solutions and is useful when the function optimized is not differentiable or when it is expected that many local optima exist. But it still requires too many CFD simulations. The gradient-based method such as adjoint method computes the derivative of the design objective with respect to the design variables to determine the search direction. Therefore, this method normally could only find the local optima, but it requires less computing load than the GA. An approach involving the solution of an adjoint system of equations has recently attracted substantial interest from mathematicians and computational scientists. Systematic mathematical and numerical analysis of optimal control problems of different types are available, such as Dirichlet, Neumann, and distributed controls, as well as finite-dimensional controls for the steady state Navier-Stokes system [6,7,8]. For the time-dependent Navier-Stokes system, Cuverlier [9] conducted a mathematical treatment of the optimal boundary for heat flux control with free convection. The existence of optimal solutions was proven, and necessary conditions were derived for characterizing optimal controls and states. Jameson [10,11] developed an adjoint approach for potential flow. He used Euler equations and Navier–Stokes equations to find the geometry that minimizes some objective function subject to a set of constraints. Gunzburger [12] built up adjoint equations and their solving method for suppression of instabilities in boundary layer flows using injection or suction control and a stress-matching problem [13]. The optimization approach solved by the adjoint method shows great potential (i.e., fast and optimal). Multiple parameters can be combined in the optimal design of ventilation in an enclosed environment.

Because of the successes in previous studies, this investigation established an adjoint method for the optimal design of indoor airflow with thermo-fluid boundary conditions as the causal aspect and flow and/or temperature fields as the design objective. By implementing this method in the CFD solver OpenFOAM (Open Field Operation And Manipulation) [14], this study determined the air-supply parameters in two, two-dimensional ventilated spaces.

2. Method

To apply the optimization approach, this study first transformed the design problem into a control problem. Then an adjoint system could be established and implemented in OpenFOAM.

2.1. Design problem as control problem

In ventilation design, the thermo-fluid boundary conditions are design variables, and flow and/or temperature fields are the design objective. Thus, the control problem consists of the following components:

- State variables: velocity V, pressure p, temperature T;
- Design variables: inlet air velocity V_{inlet} and inlet air temperature T_{inlet};
- State equations: Navier-stokes equations denoted by $S = (S_1, S_2, S_3, S_4, S_5)$ and:

$$S_1 = -\nabla \cdot V = 0 \tag{1}$$

$$(S_2, S_3, S_4)^T = (V \cdot \nabla)V + \nabla p - \nabla \cdot (2\nu D(V)) - \gamma \vec{g}(T - T_{op}) = 0 \tag{2}$$

$$S_5 = \nabla \cdot (VT) - \nabla \cdot (\kappa \nabla T) = 0 \tag{3}$$

- Objective function:

$$J(V_{inlet}, T_{inlet}) = \alpha \int_{\theta_1} (V - V_0)^2 d\theta_1 + \beta \int_{\theta_2} (T - T_0)^2 d\theta_2 \qquad (4)$$

In the state equations, S_1, S_2, S_3, S_4, and S_5 are vector components of S; ν is the effective viscosity; $D(V) = (\nabla V + (\nabla V)^T)/2$ is the rate of strain tensor; κ is the effective conductivity; T_{op} = 291.5 K that is the operating temperature; γ = 0.00343 that is the thermal expansion cofficient of the air; and $\vec{g}$ = (0, 0, 9.81) m/s^2 that is the gravity vector. In the objective function, velocity distribution V_0 on domain θ_1 and temperature distribution T_0 on domain θ_2 are the design objective, and V and T are calculated from the state function. α and β are chosen to adjust the relative importance of the two integrals in equation (4). The Boussinesq approximation is applied to simulate the thermal effect, while air density is assumed constant, which has been a common approach for room airflow simulations. Then, the optimization approach is to minimize objective function $J(V_{inlet}, T_{inlet})$ subject to the state equations.

2.2. Adjoint equations

With the introduction of a Lagrangian function L, the constrained control problem can be transformed into an unconstrained control problem. An augmented objective could be:

$$L = J + \int_{\Omega} (p_a, V_a, T_a) S d\Omega \qquad (5)$$

where Ω stands for the flow domain, V_a the adjoint velocity, p_a the adjoint pressure, and T_a the adjoint temperature. These parameters are Lagrangian multipliers. The integrand on the right hand side of Equation (5) is the dot product of vector (p_a, V_a, T_a) and vector S. Then the total variation of L is:

$$\delta L = \delta_{V_{inlet}} L + \delta_{T_{inlet}} L + \delta_V L + \delta_P L + \delta_T L \qquad (6)$$

which includes the contributions from changes in V_{inlet} and T_{inlet} and the corresponding changes in state variables V, p, and T. The state equations should be calculated once for each variable in order to satisfy $S = 0$. To find the relationship between the variations of V_{inlet} and T_{inlet} and the δL, the adjoint velocity V_a, the adjoint pressure p_a, and the adjoint temperature T_a are chosen to satisfy:

$$\delta_V L + \delta_P L + \delta_T L = 0 \qquad (7)$$

Based on equation (7), this study has developed the adjoint equations. The reader can refer to Othmer [15] for the detailed derivation procedure. In the current paper, only the adjoint equations in final form are presented, as follows:

$$-\nabla \cdot V_a = 0 \qquad (8)$$

$$-\nabla V_a \cdot V - (V \cdot \nabla) V_a - \nabla \cdot (2\nu D(V_a)) + \nabla p_a - T \nabla T_a + 2\alpha (V - V_0) = 0 \text{ for domain } \theta_1 \qquad (9)$$

$$-\nabla V_a \cdot V - (V \cdot \nabla) V_a - \nabla \cdot (2\nu D(V_a)) + \nabla p_a - T \nabla T_a = 0 \text{ for domain } \Omega \backslash \theta_1 \qquad (10)$$

$$-V\cdot\nabla T_a-\nabla\cdot(\kappa\nabla T_a)+2\beta(T-T_0)=0 \text{ for domain } \theta_2 \quad (11)$$

$$-V\cdot\nabla T_a-\nabla\cdot(\kappa\nabla T_a)=0 \text{ for domain } \Omega\backslash\theta_2 \quad (12)$$

The term $T\nabla T_a$ in Equation (9) and (10) cancels when β = 0 in the objective function. To insure the convergence of the adjoint momentuem equation, this study neglected this term in the calculations.

At the same time, this investigation has developed the corresponding adjoint boundary conditions. At the inlet and wall, the adjoint velocity boundary condition is $V_a\big|_{inlet,\, wall}=0$ and the adjoint pressure boundary condition is zero gradient. At the outlet, the adjoint velocity and pressure boundary conditions are:

$$V_{at}V_n+\nu(\vec{n}\cdot\nabla)V_{at}=0 \quad (13)$$

$$(\vec{n}\cdot\nabla)V_{an}=-\nabla_t\cdot V_{at} \quad (14)$$

$$p_a=V_a\cdot V+V_{an}V_n+\nu(\vec{n}\cdot\nabla)V_{an} \quad (15)$$

The subscripts t and n refer to the tangential and normal components, respectively. At the wall, the adjoint temperature boundary condition of zero gradient is applied. At the inlet and outlet, this study calculated the temperature as:

$$T_aV_n+\kappa(\vec{n}\cdot\nabla)T_a=0 \quad (16)$$

According to Equations (6) and (7), the variation of L is calculated as

$$\delta L=\delta_{V_{inlet}}L+\delta_{T_{inlet}}L=\delta_{V_{inlet}}J+\delta_{V_{inlet}}J+\int_{\Omega}(p_a,V_a,T_a)\delta_{V_{inlet}}Sd\Omega+\int_{\Omega}(p_a,V_a,T_a)\delta_{T_{inlet}}Sd\Omega \quad (17)$$

Thus, the sensitivity of the augmented objective becomes:

$$\frac{\delta L}{\delta V_{inlet}}=\int_{\Omega}(p_a,V_a,T_a)\frac{\partial S}{\delta V_{inlet}}d\Omega \quad (18)$$

$$\frac{\delta L}{\delta T_{inlet}}=\int_{\Omega}(p_a,V_a,T_a)\frac{\partial S}{\partial T_{inlet}}d\Omega \quad (19)$$

We set

$$\delta V_{inlet}=-\lambda_1\Big[\int_{\Omega}(p_a,V_a,T_a)\frac{\partial S}{\delta V_{inlet}}d\Omega\Big]^T \quad (20)$$

$$\delta T_{inlet}=-\lambda_2\Big[\int_{\Omega}(p_a,V_a,T_a)\frac{\partial S}{\delta T_{inlet}}d\Omega\Big]^T \quad (21)$$

where λ_1 and λ_2 are positive constants. The integrands in Equation (18) and (20) are product of a vector and a matrix, and those in Equation (17), (19), and (21) are product of two vectors. The variation of L is always negative, and the value of L always decreases until an optimum condition is achieved. Therefore, using the simple steepest descent algorithm, the variation of V_{inlet} and T_{inlet} at the boundary face cell can be written approximately as:

$$\delta V^i_{inlet} = -\lambda_1 [V^i_{inlet} \cdot V^i_{a(inlet)} - (\nabla T_{inlet})^i T_{a(inlet)}] \qquad (22)$$

$$\delta T_{inlet} = -\lambda_2 (-\gamma \vec{g} \cdot V_{a(inlet)} + \vec{n} \cdot V_{inlet} T_{a(inlet)}) \qquad (23)$$

where $V_{a(inlet)}$ and $T_{a(inlet)}$ are the calculated adjoint velocity and temperature, respectively, at the cell adjacent to the corresponding boundary face cell. The superscript i denotes a vector component.

2.3. Numerical method

Figure 1 shows that the calculation begins with an initial guessed inlet boundary condition of air velocity and temperature. With the initial boundary condition, our method first solves the state equations with N_1 iterations. Next, the method evaluates the objective function J. If J is smaller than a small constant ε set by the designer, the calculation stops, or this method initializes and calculates the adjoint equations with N_2 iterations. Based on the results of the state equations and adjoint equations, one can compute the variation of the inlet air velocity and temperature and obtain a new inlet air conditions. This creates a design cycle. After the first design cycle, the convergence criterion would be $|J-J_{old}|<\xi$ instead, where J_{old} is the computed objective function in the prior design cycle and ξ is also a small constant that set by the designer. The new boundary conditions are used to calculate the state equations again until the convergence criterion is satisfied.

N_1 and N_2 are the number of iterations for solving the state equations and adjoint equations, respectively, until they converge in each design cycle. However, N_1 and N_2 can also equal to one, where the updating of boundary conditions use partially converged state and adjoint solutions to calculate the sensitivities that is an all-at-once or one-shot method.

The solver uses a Semi-Implicit Method for Pressure-Linked Equations (SIMPLE) [16] algorithm to couple the velocity/adjoint velocity and pressure/adjoint pressure in solving the state/adjoint equations.

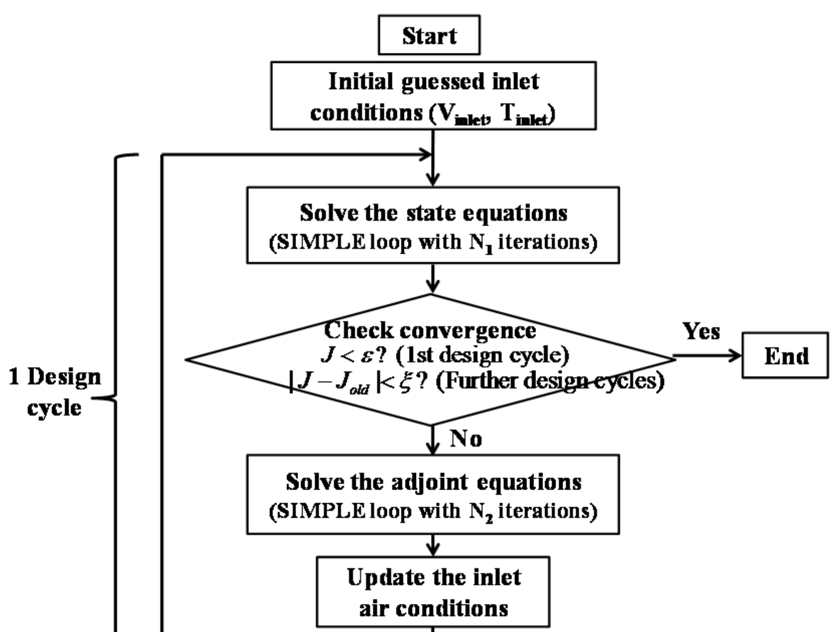

Figure 1. Solution flow chart for the adjoint method

This investigation applied the standard k-ε model [17] to simulate turbulence in the state equations. To decrease the calculation load, this study assumed the turbulence to be "frozen" [15,18], and the turbulent viscosity in the state equations was re-used for the adjoint diffusion term. For the convection terms, this study adopted the standard finite volume discretisation of Gaussian integration with the first-order upwind-differencing-interpolation (Gauss Upwind) scheme [19]. The diffusion terms adopted the standard finite volume discretisation of Gaussian integration with the central-differencing-interpolation (Gauss Linear) scheme. The adjoint equations applied the Gauss Linear scheme for the gradient term. Neither the Gauss upwind scheme nor the Gauss liner scheme is the most accurate, but these two schemes can make the calculation stable. This investigation solved the state and adjoint continuity equations by the generalized Geometric-Algebraic Multi-Grid (GAMG) [20] solver. GAMG is faster than standard methods when the increase in speed by solving first on coarser meshes outweighs the additional costs of mesh refinement and mapping of field data. The adjoint method was implemented in OpenFOAM, which is a CFD toolbox and can be used to simulate a broad range of physical problems.

3. Results

This study has validated the adjoint method by applying it to two, two-dimensional ventilation cases, one with isothermal flow and the other with non-isothermal flow.

3.1. Isothermal case

This case was from Nielsen [21], who provided detailed experimental data. As the inlet air temperature and the wall temperature were identical and no heat sources in the cavity, it is an isothermal case as the temperature is uniform thoroughout the cavity. Therefore, this study did not considered the energy equation and adjoint adjoint equation in this case. Figure 2 shows the geometry of this case, where L/H=3.0, h/H=0.056, and t/H=0.16, and where H=3.0 m. It also shows the mesh used in the calculations. The inlet velocity was V_x=0.455 m/s and V_y=0 with a turbulence intensity(TI) of 4% that is computed by [22]:

$$TI = V' / \overline{V} = \sqrt{\frac{1}{3}(V_x'^2 + V_y'^2 + V_z'^2)} / \overline{V} \qquad (24)$$

where the prime denotes the turbulent fluctuation and the bar denotes the averaged value.

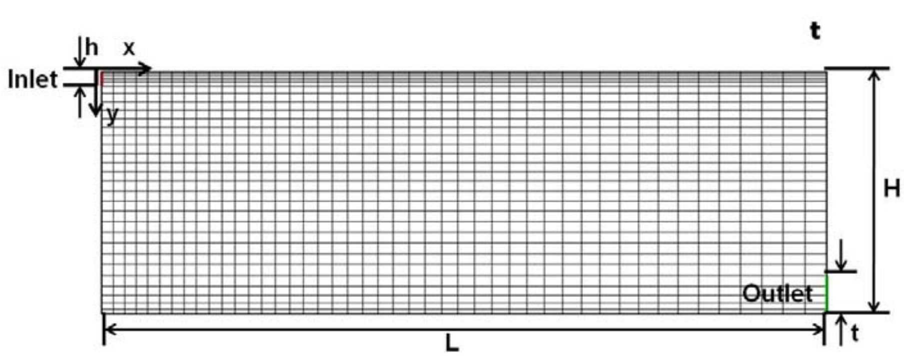

Figure 2. Sketch and mesh of the two-dimensional isothermal case.

This study first conducted a forward CFD simulation with the standard k-ε model by assigning the inlet air velocity as V_x=0.455 m/s and V_y=0 corresponding to Reynolds number (Re):

$$\mathrm{Re} = \frac{hV_x}{\nu} = 5000 \tag{25}$$

where kinematic viscosity ν for air is 15.3 × 10^{-6} m^2/s in this case. The forward CFD simulation was performed to obtain a flow field in the room, and a section of it can be used as the design objective. Figure 3 shows the computed air velocity profile (V_0 in Equation (4)) at the lower section of line x=6 m (design domain θ_1) that was selected as the design objective. So in the objective function (Equation (4)), this study set α = 1 and β = 0. Next, this study aimed to find the optimal inlet air velocity based on this design objective. As the design objective was produced by the assigned inlet air velocity of V_x = 0.455 m/s and V_y = 0, this value is the most optimal and the optimized inlet air velocity may be the same as this value. However, the solution may lead to other values as long as the objective is reached.

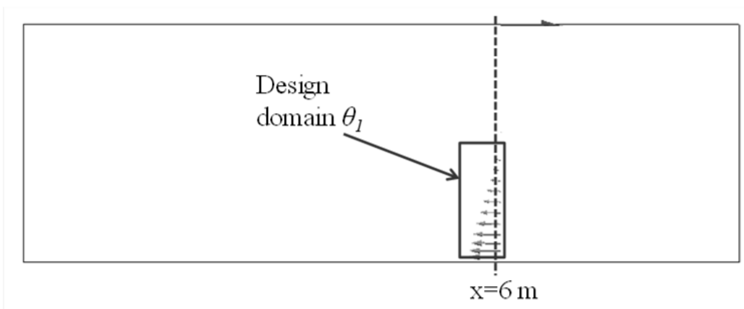

Figure 3. Design objective for the two-dimensional isothermal case

Because the isothermal case was simple, the adjoint method could lead to a converged solution in a limited number of iterations. For simplicity, this study used N_1=N_2=1 (see Figure 1) in the calculation. This investigation used four different inlet air velocities as the initial inlet conditions, which were different from the true value of V_x = 0.455 m/s and V_y = 0.0 m/s:

(1) V_x = 1.0 m/s and V_y = 0.0 m/s
(2) V_x = 1.0 m/s and V_y = 0.1 m/s
(3) V_x = 1.0 m/s and V_y = -0.1 m/s
(4) V_x = 1.0 m/s and V_y = 0.3 m/s

With the initial boundary conditions, the flow and adjoint equations were calculated for 2000 design cycles with N_1=N_2=1. Figures 4 and 5 show that the first three initial conditions gradually changed to the true result of V_x = 0.455 m/s and V_y = 0.0 m/s. The error for V_x was as small as 0.25-1.8%. The error for V_x was as small as 0.25-1.8%, and the calculated V_y was exactly 0.0 m/s. Unexpectedly, the calculation with an initial velocity of V_x = 1.0 m/s and V_y = 0.3 m/s led to a final velocity of V_x = 0.132 m/s and V_y = 2.578 m/s. Figure 6 further shows that all the calculations could lead to a small value of the objective function. Figures 4-6 illustrate that the calculations at the beginning were unstable. This was caused by the partially converged flow field and adjoint equations as N_1=N_2=1. The calculation was also unstable when the cycle number equalled 500, and it was difficult to identify the exact cause.

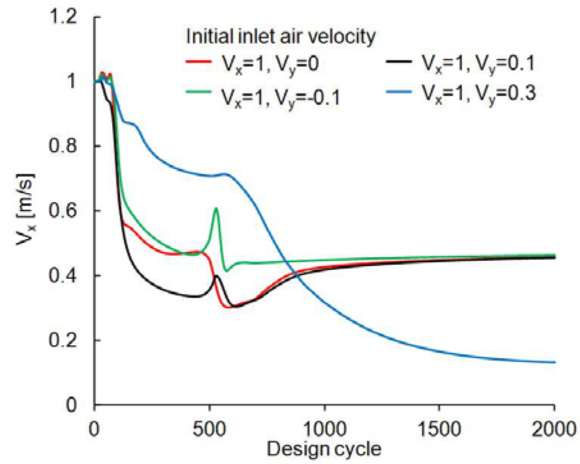

Figure 4. Change in V_x with the design cycle

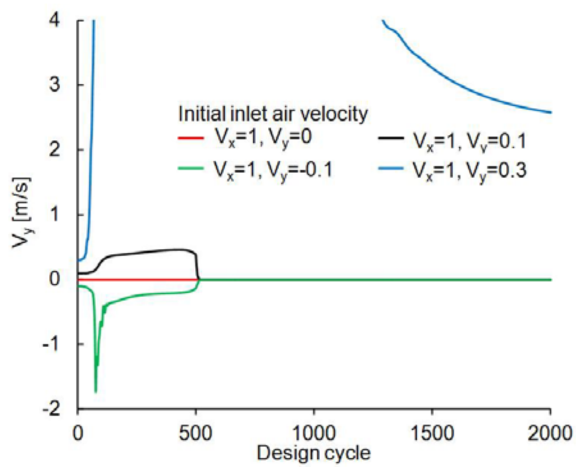

Figure 5. Change in V_y with the design cycle

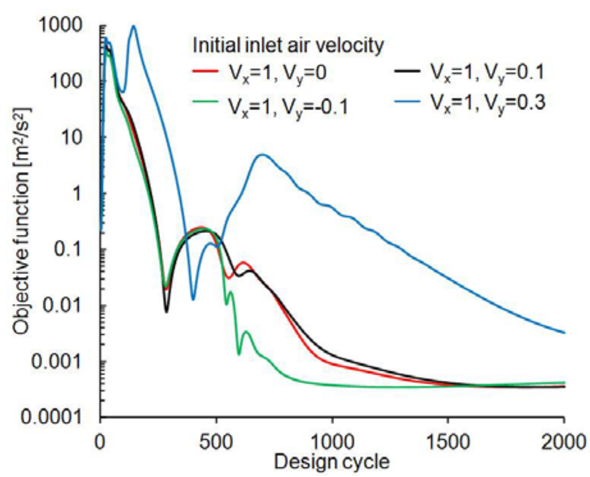

Figure 6. Change in the objective function with the design cycle

This study then conducted forward CFD simulations with the inlet air velocities determined by the adjoint method. Figure 7 compares the computed velocity profiles at x = 6 m with the profile computed by the exact inlet air velocity of V_x=0.455 m/s and V_y=0 m/s. Only the calculation with an inlet velocity of V_x=0.132 m/s and V_y = 2.578 m/s displayed a minor difference. Therefore, this adjoint method can find the optimal inlet air velocity with a small value of the objective function. In other words, the adjoint method can inversely find the desired inlet air velocity by setting the velocity profile in the lower part of x = 6 m as the design objective. However, the results show that in order to achieve the design objective, the solution may not be unique.

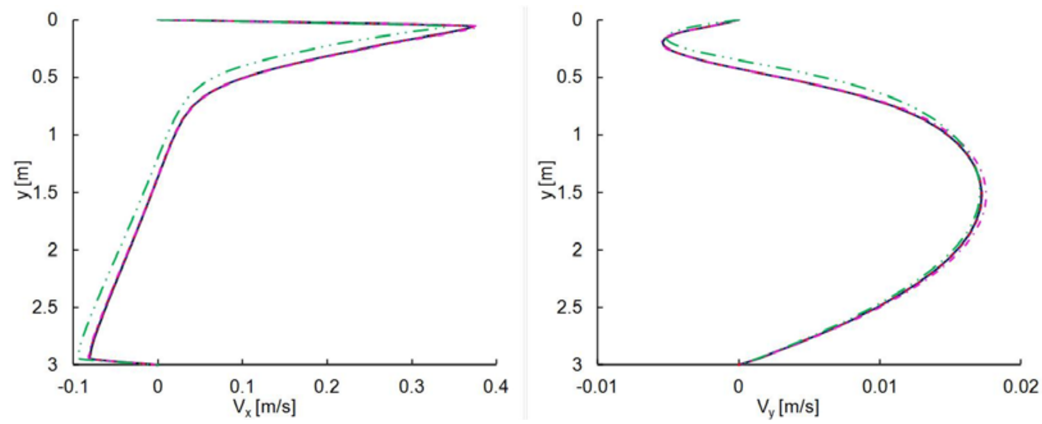

(a) Comparison of V_x at x = 6 m (b) Comparison of V_y at x = 6 m

With exact inlet condition of V_x=0.455, V_y=0

With inlet condition determined with initial inlet condition of V_x=1, V_y=0

With inlet condition determined with initial inlet condition of V_x=1, V_y=0.1

With inlet condition determined with initial inlet condition of V_x=1, V_y=-0.1

With inlet condition determined with initial inlet condition of V_x=1, V_y=0.3

Figure 7. Comparison of the design objective (velocity profiles) determined by the adjoint method and that determined by the specified inlet condition of V_x = 0.455 m/s, V_y = 0 m/s at x = 6 m.

3.2. Non-isothermal case

This investigation also applied the adjoint method to a two-dimensional, non-isothermal case as shown in Figure 8. The dimensions of the flow domain were 1.04 m × 1.04 m, the inlet height was h = 18 mm, and the outlet height was t = 24 mm. The inlet air velocity was V_x = 0.57 m/s, V_y = 0.0 m/s, and the inlet air temperature (T_{inlet}) was 15ºC. The temperature of the walls (T_{wall}) was 15ºC, and that of the floor (T_{fl}) was 35ºC. Figure 8 also shows the resolution of the mesh used in the numerical simulation. Blay et al. [23] conducted experimental measurements of the airflow and temperature distributions for this case.

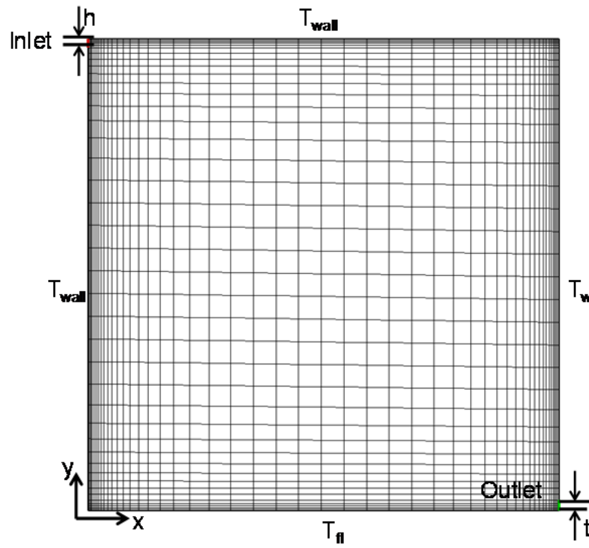

Figure 8. Sketch and mesh of the two-dimensional, non-isothermal case.

Again, this study conducted a CFD simulation with inlet air velocity V_x =0.57 m/s and V_y = 0.0 and inlet air temperature of 15ºC to generate a design objective. The design objective selected for this case was the air velocity profile (V_0 in Equation (4)) and/or air temperature profile (T_0 in Equation (4)) at mid-cavity (design domain $\theta_1 = \theta_2$) as shown by the red line in Figure 9:

Scenario 1: Air velocity profile
Scenario 2: Air temperature profile
Scenario 3: Air velocity and temperature profiles

The design variables were the inlet air temperature and velocity. For Scenario 3, to adjust the importance of the velocity error and temperature error in the objective function, this study normalized the velocity error by the exact inlet air velocity V_x = 0.57 m/s and the temperature error by (T_{fl} - T_{inlet}). So we have:

$$\alpha = \frac{1}{V_x^2};\ \beta = \frac{1}{(T_{fl} - T_{inlet})^2} \tag{26}$$

Table 1 summarized the intial inlet air conditions for each scenario:

Table 1. Initial inlet air conditions for each scenario.

	Case	Initial inlet air temperature (ºC)	Initial inlet air velocity (m/s)
Scenario 1	1a	T = 6.85	V_x = 1.0, V_y = 0.5
	1b	T = 21.85	
Scenario 2	2a	T = 6.85	
	2b	T = 21.85	
Scenario 3	3a	T = 6.85	
	3b	T = 21.85	

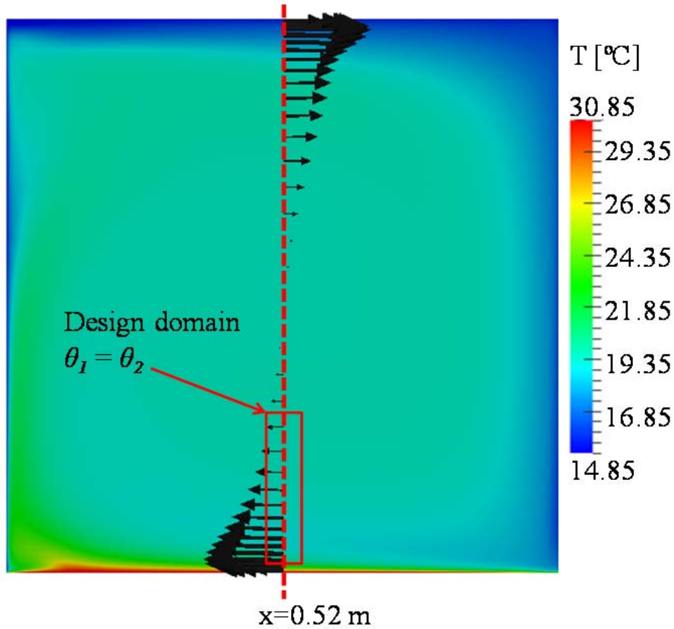

Figure 9. Design objective for the two-dimensional, non-isothermal case: velocity and/or temperature profiles at mid-cavity as shown by the red line.

Since this was a non-isothermal case, the adjoint method also solved the energy equation. Without iterations (N_1=N_2=1), the solution would have diverged as a result of highly significant and sometimes unreasonable changes in the variables. Therefore, this study set N_1=N_2>1 (see the solution flow chart) in the calculations in order to achieve a stable and converged solution.

3.2.1. Scenario 1: Using air velocity as the objective. For this scenario, this study initialized the inlet velocity and temperature as V_x = 1 m/s, V_y = 0.5 m/s, and T = 6.85 ºC as Case 1a and V_x = 1 m/s, V_y = 0.5 m/s, and T = 21.85 ºC as Case 1b. Furthermore, this investigation used N_1=N_2=100 for each design cycle and conducted 100 design cycles. Figure 10 shows that the objective function was as small as 10^{-3} at the end of the calculation, indicating that an optimal design had been reached. However, the two initial conditions led to two different optimal inlet conditions. Figure 10(a) shows a final inlet air velocity of V_x = 0.563 m/s and V_y = 0.007 m/s and a final inlet air temperature of T = 14.85ºC. The final condition was very close to the true inlet condition of V_x =0.57 m/s, V_y = 0 m/s, and T = 15ºC. However, Figure 10(b) shows a final inlet condition of V_x = 0.755 m/s, V_y = 0.254 m/s, and T = 21.85ºC, which is quite different. Because only the velocity field was used as the design objective, multiple optimal solutions could exist.

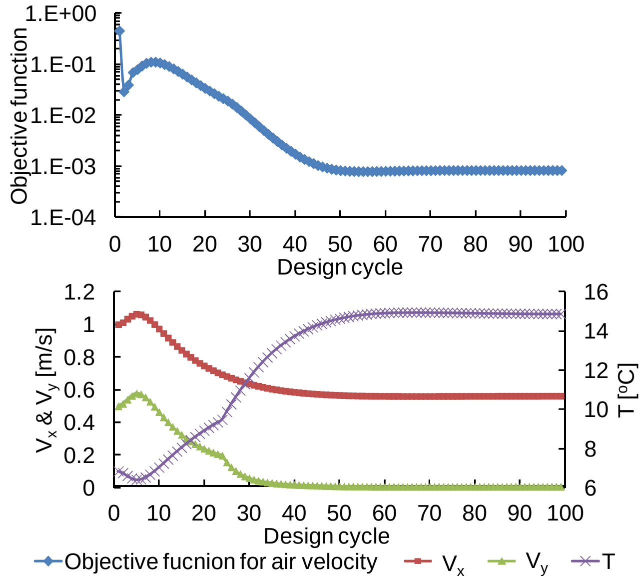

(a) Case 1a with initial inlet condition of V_x = 1 m/s, V_y = 0.5 m/s, and T = 6.85ºC

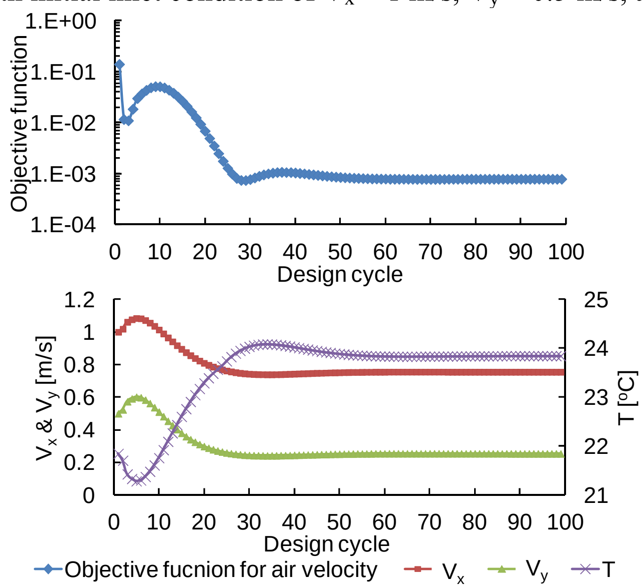

(b) Case 1b with initial inlet condition of V_x = 1 m/s, V_y = 0.5 m/s, and T = 21.85ºC

Figure 10. Changes in V_x, V_y, and T at the inlet and the objective function with the number of design cycles, with partial flow field as design objective.

As in the isothermal case, this study also conducted forward CFD simulations with final inlet air velocity and temperature determined by the adjoint method. Figure 11 compares the computed velocity profiles at mid-cavity (x = 0.52 m) with that using the exact inlet condition of V_x =0.57 m/s, V_y = 0 m/s, and T = 15 ºC. It can be seen that the two final inlet conditions had almost the same velocity profiles as the design objective.

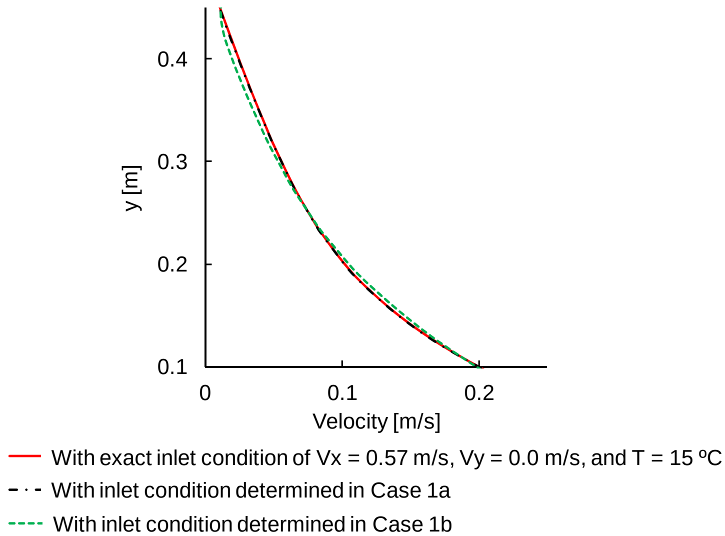

Figure 11. Comparison of the design objective (velocity profiles) determined by the adjoint method and that determined by the specified inlet condition of V_x =0.57 m/s, V_y = 0 m/s, and T = 15ºC at x=0.52 m.

3.3.2. Scenario 2: Using air temperature as the objective. Since it is much harder to obtain a converged result after adding the energy equation into the adjoint method, N_1 and N_2 were set at 5000. This study again initialized the inlet velocity and temperature as V_x = 1 m/s, V_y = 0.5 m/s, and T = 6.85 ºC as Case 2a and V_x = 1 m/s, V_y = 0.5 m/s, and T = 21.85 ºC as Case 2b. Figure 12 shows that, the objective function decreased gradually to about 0.02 in 60 design cycles. Then the corresponding average temperature difference between the temperature design objective and the calculated temperature distribution in the lower part of the mid-cavity was about 0.01 K. However, the optimal inlet air conditions are V_x = 0.324 m/s, V_y = 0.477 m/s, and T = 12.44 ºC for Case 2a and V_x = 0.870 m/s, V_y = 0.482 m/s, and T = 16.47 ºC for Case 2b, which are quite different from the true value of V_x =0.57 m/s, V_y = 0 m/s, and T = 15 ºC. This study also tried some other initial conditions, and the calculation always approached optimal solutions that differed from the true value, although the objective function became as small as 10^{-2}. Because different inlet conditions can lead to similar temperature distributions in the lower part of the mid-cavity, multiple optimal solutions are not a complete surprise to us.

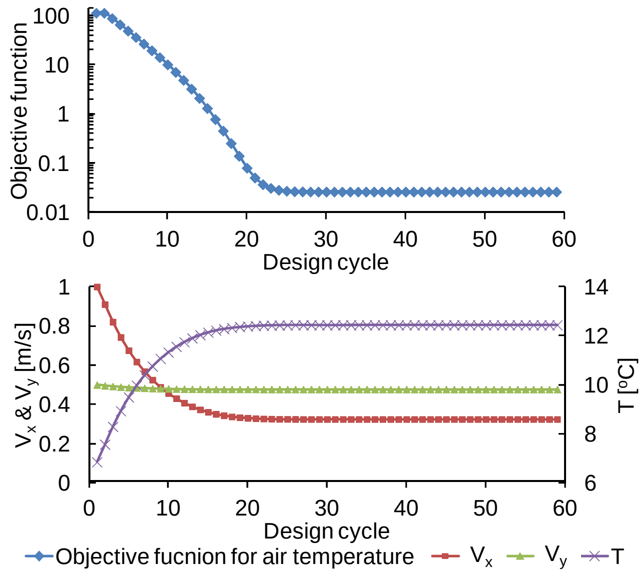

(a) Case 2a with initial inlet condition of V_x = 1 m/s, V_y = 0.5 m/s, and T = 6.85ºC

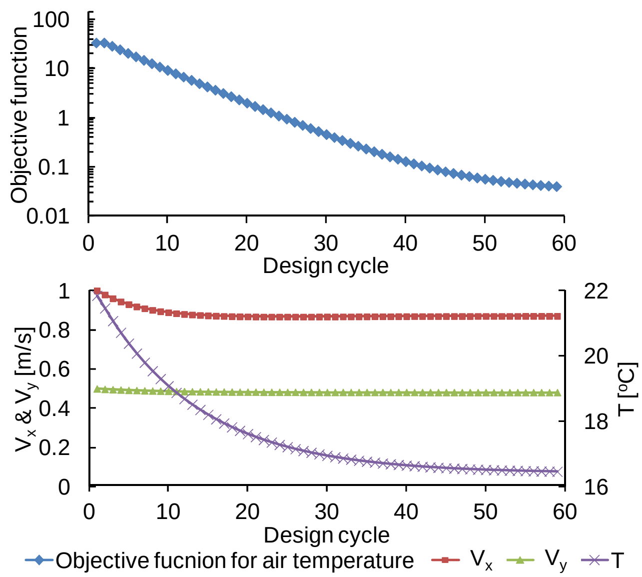

(b) Case 2b with initial inlet condition of V_x = 1 m/s, V_y = 0.5 m/s, and T = 21.85ºC

Figure 12. Changes in V_x, V_y, and T at the inlet and objective function with the number of design cycles, with partial temperature field as design objective.

3.3.3. Scenario 3: Using air velocity and temperature as the objective. The design objective in Scenario 3 is to satisfy the air velocity and temperature profile in the lower part of the mid-cavity. This study again used an initial inlet condition of V_x = 1 m/s, V_y = 0.5 m/s, and T = 6.85ºC as Case 3a, and a condition of V_x = 1 m/s, V_y = 0.5 m/s, and T = 21.85ºC as Case 3b. N_1 and N_2 were set at 1000, which is a trade-off between the convergence of the calculations and computing effort. For each condition, this study calculated no more than 400 design cycles. Figure 13 shows that the final thermo-fluid boundary condition at the inlet for Case 3a was V_x = 0.528 m/s, V_y = 0.109 m/s, and T = 14.63 ºC, and for Case 3b it was V_x = 0.537, V_y = 0.084 m/s, and T = 14.68ºC. The two final inlet conditions agree well with the true condition at the inlet as V_x =0.57 m/s, V_y = 0 m/s, and T = 15 ºC. It seems that the optimal solution was unique when both the air velocity and temperature profiles were specified as the design objective.

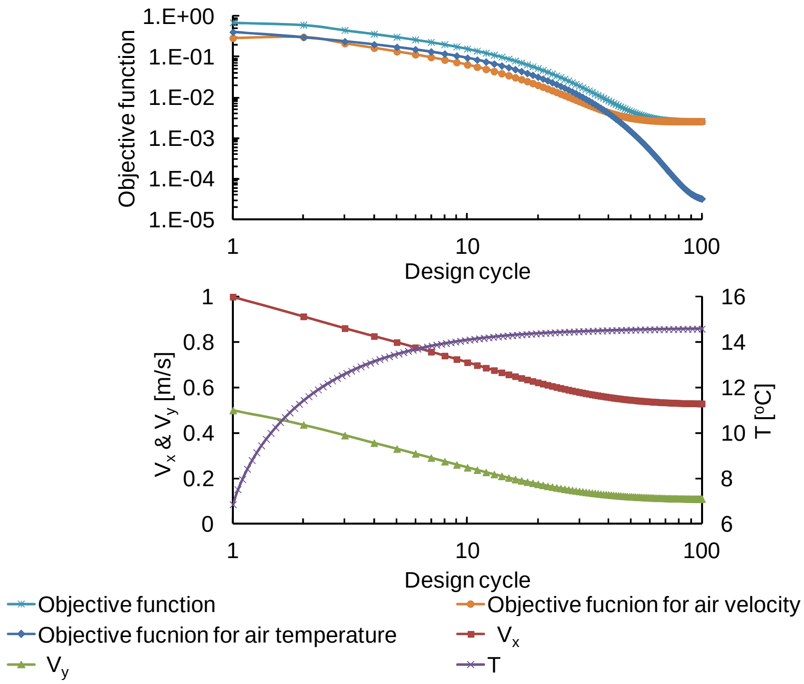

(a) Case 3a with initial inlet condition of V_x = 1 m/s, V_y = 0.5 m/s, and T = 6.85ºC

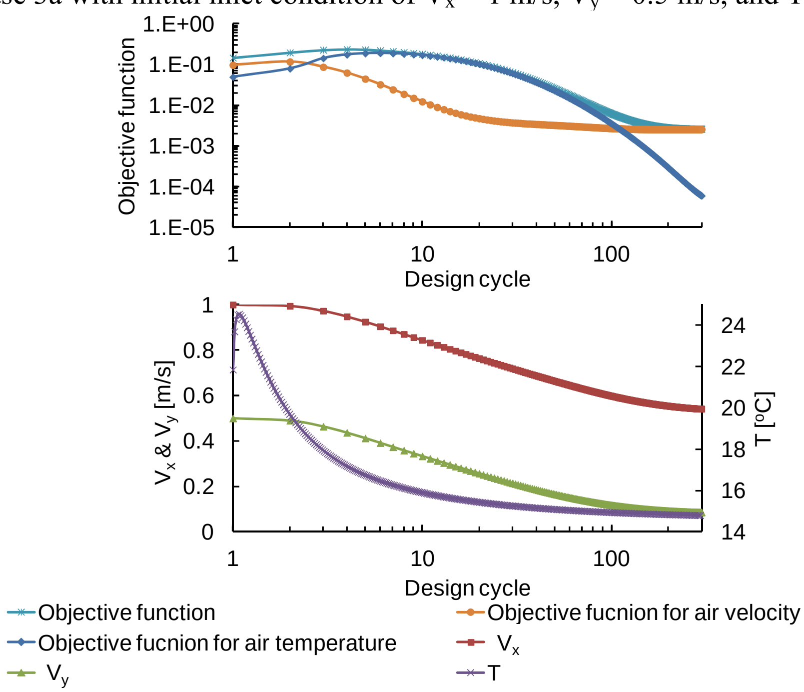

(b) Case 3b with initial inlet condition of V_x = 1 m/s, V_y = 0.5 m/s, and T = 21.85ºC

Figure 13. Changes in V_x, V_y, and T at the inlet and design objective with the number of design cycles, with partial flow and temperature fields as design objective.

Figure 13 also shows that the objective function for air velocity became 10^{-3} and that for air temperature became 10^{-2}. The corresponding average velocity in the lower part of the mid-cavity differed by only 0.003 m/s from the design objective, and the average air temperature differed by only 0.01 K from the design objective.

4. Discussions

In the isothermal case, within 1 iteration/cycle × 2000 cycles, the adjoint method could find the optimal inlet air velocity. The calculation time was roughly twice that required by forward CFD simulation for 4000 iterations (no internal iteration) in solving the flow. However, in Scenario 3 of the non-isothermal case, the adjoint method could also find the optimal inlet conditions in 1,000 iterations/cycle × 400 design cycles. The more complex flow can increase the computing effort by one or two magnitudes.

In addition, the more design objectives there are, such as in Scenario 3, the lower the likelihood that multiple solutions will occur. It is possible that if too many design objectives are specified, then no solution can be obtained.

This study aimed to verify the applicability of the adjoint method in the optimal design of indoor environment, so the design variables were only the inlet air velocity and temperature. The former investigations [10, 11] showed that this method should work with more design variables. However, the design variables in this study are of different types (velocity and temperature) that are different from the application of this adjoint in other areas. This study verified the inverse identification of design variables in different types.

This is our first approach that inversely designs the indoor environment. The objective functions were only the partial air velocity and temperature profiles, the design variables were only the inlet air velocity and temperature, and the cases for validation were two-dimensional. We are rather happy to have achieved the goals set. Based on the results obtained in this study, our future work will continue on the following three aspects: (1) more design variables such as inlet location and size, and the interior furnishings, etc.; (2) expansion to three-dimensional and more challenging cases such as an office or an aircraft cabin; and (3) more challenging design objectives, such as thermal comfort, indoor air quality, and energy efficiency, etc.

5. Conclusions

This investigation developed an adjoint method and implemented it in OpenFOAM to determine the optimal thermo-fluid boundary conditions for designing the best indoor environment. By applying the method to solve the inlet conditions with air velocity and/or air temperature in rooms as the design objective, the inlet conditions could be inversely identified.

For the isothermal case, this study used a velocity profile in the lower part of the room computed by a forward CFD simulation as the design objective. The results showed that this adjoint method could accurately find the optimal inlet air velocity by using different initial inlet conditions. However, the calculations with different initial inlet air conditions led to different optimal inlet air conditions, which implies the existence of multiple solutions.

For the non-isothermal case, when only the air velocity profile or only the air temperature profile in the lower part of the mid-cavity was used as the design objective, the calculation led to multiple solutions. When both the air velocity and temperature profiles were used as the design objective, the calculations with different initial inlet air conditions found a unique solution for the inlet condition.

Nomenclature

Symbol definition

D	rate of strain tensor
$\vec{g}$	gravity vector, m·s^{-2}
J	objective function
L	augmented objective function
$\vec{n}$	unit vector in the normal direction
N	iteration numbers
p	pressure, Pa
Re	Reynolds number
S	Navier-stokes equations vector form
T	temperature, ºC
TI	turbulence intensity
V	velocity, vector, m·s^{-1}
x, y	index of coordinates

Subscripts

0	design objective
a	adjoint parameter
fl	value at the floor
i	component of a vector
inlet	value at the inlet
n	normal component
old	value at prior design cycle
op	operating value
t	tangential component
wall	value at the wall
x	component in the x direction
y	component in the y direction

Superscripts

i	component of a vector
T	transpose

Greek symbols

α	positive constant
β	positive constant
γ	thermal expansion cofficient
δ	variation
ε	positive constant
θ	design domain
κ	effective conductivity
λ	positive constant
ν	effective viscosity
ξ	positive constant
Γ	effective diffusivity
Ω	flow domain

Acknowledgements

The research presented in this paper was partially supported by the National Basic Research Program of China (the 973 Program) through Grant No. 2012CB720100.

References

[1] ASHRAE, *Ventilation for acceptable indoor air quality*, Atlanta, GA, 2007.

[2] Q. Chen, Ventilation performance prediction for buildings: A method overview and recent applications, *Building and Environment*, 44(4), 848-858, 2009.

[3] S. M. Gorelick, B. E. Evans, and I. Remson, Identifying sources of groundwater pollution: an optimization approach, *Water Resources*, 19(3), 779-790, 1983.

[4] B. J. Wagner, Simultaneously parameter estimation and contaminant source characterization for coupled groundwater flow and contaminant transport modelling, *Journal of Hydrology*, 135, 275-303, 1992.

[5] P. S. Mahar and B. Datta, Identification of pollution sources in transient groundwater system, *Water Resource Management*, 14(6), 209-227, 2000.

[6] M. Gunzburger, L. Hou, and T. Svobodny, Numerical approximation of an optimal control problem associated with the Navier-Stokes equations, *Applied Mathematics*, 2, 29-31, 1989.

[7] M. Gunzburger, L. Hou, and T. Svobodny, Analysis and finite element approximation of optimal control problems for the stationary Navier-Stokes equations with distributed and Neumann controls, *Mathematics of Computation*, 57, 123-151, 1991.

[8] M. Gunzburger, L. Hou, and T. Svobodny, Boundary velocity control of incompressible flow with an application to viscous drag reduction, *SIAM Journal on Control and Optimization*, 30, 167-181, 1991.

[9] P. Cuverlier, Optimal control of a system governed by the Navier-Stokes equations coupled with the heat equation, *New Developments in Differential Equations*, W. Eckhaus, ed., North-Holland, Amsterdam, 81-98, 1976.

[10] A. Jameson, Aerodynamic design via control theory, *Journal of Scientific Computing*, 3, 233-260, 1988.

[11] A. Jameson, Optimum aerodynamic design using CFD and control theory, *AIAA 12th Computational Fluid Dynamics Conference*, San Diego, CA, 1995-1729, 1995.

[12] M. Gunzburger, Sensitivities, adjoints and flow optimization, *International Journal for Numerical Methods in Fluids*, 31, 53-78, 1999.

[13] R. Joslin, M. Gunzburger, R. Nicolaides, G. Erlebacher, and M. Hussaini. An automated methodology for optimal flow control with an application to transition delay, *AIAA Journal*, 35, 816-824, 1997.

[14] OpenFOAM, The Open Source CFD Toolbox, http://www.opencfd.co.uk/openfoam.html, 2007.

[15] C. Othmer, A continuous adjoint formulation for the computation of topological and surface sensitivities of ducted flows, International Journal for Numerical Methods in Fluids, 58, 861-877, 2008.

[16] S. V. Patankar and D. B. Spalding, A calculation procedure for heat, mass and momentum transfer in three-dimensional parabolic flows. *International Journal of Heat and Mass Transfer*, 15(10), 1787-1806, 1972.

[17] B. Launder and B. Sharma, Application of the energy-dissipation model of turbulence to the calculation of flow near a spinning disc, *Letters in Heat Mass Transfer*, 1, 131-138, 1974.

[18] R. P. Dwight and J. Brezillon, Effect of various approximations of the discrete adjoint on gradient-based optimization, *Proceedings of the 44th AIAA Aerospace Sciences Meeting and Exhibit*, Reno, NV, 2006.

[19] J. B. Scarborough, Numerical mathematical analysis. Oxford and IBH Publishing, 1955.

[20] W. Hackbusch, Multi-grid methods and applications (Vol. 4). Berlin: Springer-Verlag, 1985.

[21] P. V. Nielsen, A. Restivo, and J. H. Whitelaw, The velocity characteristics of ventilated rooms, *Journal of Fluids Engineering*, 100, 291-298, 1978.
[22] http://www.cfd-online.com/Wiki/Turbulence_intensity.
[23] D. Blay, S. Mergui, and C. Niculae, Confined turbulent mixed convection in the presence of a horizontal buoyant wall jet, Fundamentals of Mixed Convection, *ASME HTD*, 213, 65-72, 1992.